Predictive Value of Metabolic Parameters Derived From ^{18}F-FDG PET/CT for Microsatellite Instability in Patients With Colorectal Carcinoma

Hao Liu[1,2†], Zheng Ye[1†], Ting Yang[1†], Hongjun Xie[2], Ting Duan[1], Mou Li[1], Min Wu[1*] and Bin Song[1*]

[1] Department of Radiology, West China Hospital, Sichuan University, Chengdu, China, [2] Department of Nuclear Medicine, Sichuan Academy of Medical Sciences, Sichuan Provincial People's Hospital, Chengdu, China

Background: Microsatellite instability (MSI) is one of the important factors that determine the effectiveness of immunotherapy in colorectal cancer (CRC) and serves as a prognostic biomarker for its clinical outcomes.

Purpose: To investigate whether the metabolic parameters derived from ^{18}F-fluorodeoxyglucose (^{18}F-FDG) positron emission tomography/computed tomography (PET/CT) can predict MSI status in patients with CRC.

Materials and Methods: A retrospective analysis was performed on CRC patients who underwent ^{18}F-FDG PET/CT examination before surgery between January 2015 and April 2021. The metabolic ^{18}F-FDG PET/CT parameters of the primary CRC lesion were calculated and recorded with different thresholds, including the maximum, peak, and mean standardized uptake value (SUV_{max}, SUV_{peak}, and SUV_{mean}), as well as the metabolic tumor volume (MTV) and the total lesion glycolysis (TLG). The status of MSI was determined by immunohistochemical assessment. The difference of quantitative parameters between MSI and microsatellite stability (MSS) groups was assessed, and the receiver operating characteristic (ROC) analyses with area under ROC curves (AUC) was used to evaluate the predictive performance of metabolic parameters.

Results: A total of 44 patients (24 men and 20 women; mean ± standard deviation age: 71.1 ± 14.2 years) were included. There were 14 patients in the MSI group while there were 30 in the MSS group. $MTV_{30\%}$, $MTV_{40\%}$, $MTV_{50\%}$, and $MTV_{60\%}$, as well as $TLG_{50\%}$ and $TLG_{60\%}$ showed significant difference between two groups (all p-values <0.05), among which $MTV_{50\%}$ demonstrated the highest performance in the prediction of MSI, with an AUC of 0.805 [95% confidence interval (CI): 0.657–0.909], a sensitivity of 92.9% (95% CI: 0.661–0.998), and a specificity of 66.7% (95% CI: 0.472–0.827). Patients' age and $MTV_{50\%}$ were significant predictive indicators of MSI in multivariate logistic regression.

Conclusion: The metabolic parameters derived from ^{18}F-FDG PET/CT were able to preoperatively predict the MSI status in CRC, with $MTV_{50\%}$ demonstrating the highest predictive performance. PET/CT imaging could serve as a noninvasive tool in the guidance of immunotherapy and individualized treatment in CRC patients.

Keywords: PET/CT, metabolism, colorectal carcinoma, microsatellite instability, immunotherapy

INTRODUCTION

Colorectal cancer (CRC) is the third most common cancer and one of the major causes of cancer-associated mortality worldwide (1). Multiple treatments for primary and metastatic CRC have emerged, which includes curative surgery, radiotherapy, neoadjuvant chemotherapy, and immunotherapy (2). Immunotherapy is a treatment option that utilizes the body's own immune system to attack cancer cells (3). Blocking immune checkpoints is currently one of the most promising approaches to activate therapeutic anti-tumor immunity and has shown encouraging results in CRC therapy (4).

However, the strong heterogeneity of CRC often leads to different prognosis and clinical outcome in patients who received similar treatment (5). As previously reported, chromosomal and genetic alterations that occur during the pathogenesis of CRC may be one of the contributing factors of heterogeneity (6). Microsatellites are short tandem repeat DNA sequences of one to three base pairs distributed throughout the human genome. Owing to their repeated structure, microsatellites are particularly prone to replication errors that are normally repaired by the mismatch repair (MMR) system. Microsatellite instability (MSI), caused by the absence of one or more MMR genes, has been considered as a reliable biomarker in the prediction of treatment response and prognosis in patients with CRC. Passardi et al. found that CRC with MSI selectively displayed highly upregulated expression of multiple immune checkpoints, including programmed death-1 (PD-1) and programmed death-ligand 1 (PD-L1) (7). In other words, CRC with MSI seem to be particularly responsive to immunotherapy, such as anti-PD-1 or anti-PD-L1 drugs. Moreover, MSI was identified as an important indicator in the selection of chemotherapy drugs of CRC (8). Recent studies showed that CRC with MSI was resistant to 5-fluorouracil (5-FU) chemotherapy and did not benefit from it (9). Typically speaking, MSI status is assessed with pathological specimen after surgery or biopsy, which is invasive and subject to sampling error (10). Therefore, a noninvasive method is urgently needed to preoperatively evaluate the MSI status and better facilitate the immunotherapy of CRC patients.

Medical imaging can capture information about the heterogeneity of the entire tumor noninvasively and could well predict tumor subtypes and the sensitivity of immunotherapy (11, 12). Moreover, imaging biomarkers were reported to be one of the effective indicators for predicting MSI expression in CRC (13–15). Wu et al. found that the quantitative imaging features derived from dual-energy computed tomography (DECT) showed good predictive performance for MSI status in CRC patients (13). In addition, radiomics-based artificial intelligence (AI), such as MRI-based deep learning models, also demonstrated

optimal diagnostic capability for discriminating MSI from microsatellite stability (MSS) (14). However, the abovementioned studies either failed to reflect tumor metabolism or entailed complicated procedure, which was unavailable in clinical practice yet. Positron emission tomography/computed tomography (PET/CT) is a molecular imaging technique that can reflect tumor microenvironment and metabolic information with clinical radiotracer, such as ^{18}F-fluorodeoxyglucose (^{18}F-FDG) (16). A recent study showed that glucose metabolic response could predict anti-PD-1 therapeutic response in lung cancer (17). However, the role of metabolic parameters in CRC and MSI predictions remained unknown. Therefore, the purpose of this study was to investigate whether metabolic parameters derived from ^{18}F-FDG PET/CT can predict MSI status in patients with CRC.

MATERIALS AND METHODS

Patients

This retrospective study was approved by the Institutional Review Board of our institution, and the written informed consent was waived. We screened the medical records of patients who underwent preoperative ^{18}F-FDG PET/CT followed by curative operations for CRC at our institution between January 2015 and April 2021. Detailed inclusion criteria were as follows: patients with (a) primary colorectal lesions diagnosed as colorectal adenocarcinoma by pathology; (b) complete preoperative whole body ^{18}F-FDG PET/CT images before surgery within 3 months; (c) adequate immunohistochemical staining for the assessment of MMR protein expression.

We initially included 92 patients, and patients (a) who received neoadjuvant chemoradiotherapy (CRT) before ^{18}F-FDG PET/CT examination ($n = 10$); (b) without complete surgical pathology records ($n = 27$) or immunohistochemical assessment ($n = 2$); and (c) diagnosed as other pathological types ($n = 9$) were excluded (**Figure 1**).

PET/CT Acquisition Protocol

All patients were asked to fast at least 8 h before the examination. In patients with diabetes, antihyperglycemic drugs were requested to stop for 12 h before the exam. The blood glucose of patients was tested before the injection of ^{18}F-FDG, and the blood glucose level was required to be lower than 8 mmol/L. Patients were intravenously administered 5.5 MBq/kg ^{18}F-FDG and received PET/CT examination after 1 h rest.

FIGURE 1 | The flowchart of patient inclusion and exclusion.
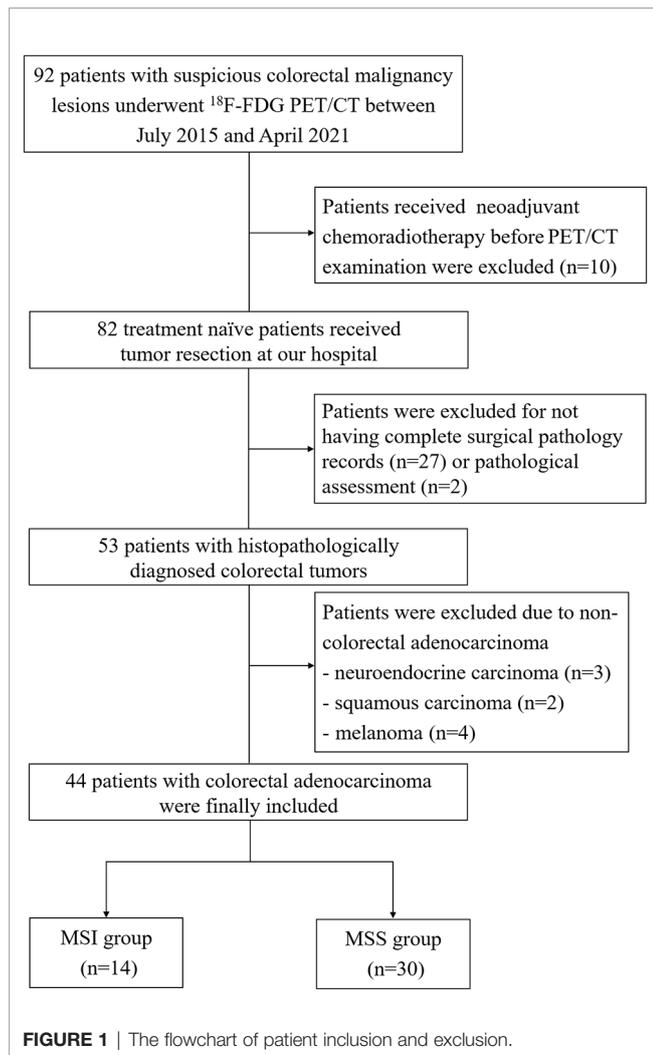
PET/CT examination was performed with a hybrid scanner (Biograph Duo or Biograph mCTFlow64-4R, Siemens Healthcare Solutions Knoxville, TN). A non-contrast CT scan was firstly performed for localization and attenuation correction, with a slice thickness of 5 mm, a tube voltage of 120 kV, and tube current depending on the patient's weight. Afterwards, PET images were acquired from the base of the skull to the proximal thigh for 3 min per bed position in a three-dimensional mode (Biograph Duo), or continuous table motion acquisitions (Biograph mCT Flow 64-4R). PET images were then reconstructed with an ordered method of ultra HD-PET, which included time of flight (TOF) and resolution recovery (TrueX) information.

Image Analysis

All PET/CT images were analyzed by using Syngo TrueD VE40E workstation (Siemens Medical Solutions). The primary lesions were identified and analyzed by two experienced independent nuclear physicians who were blinded to any clinical and pathological information. Malignant lesions typically showed higher ^{18}F-FDG concentration than that of the surrounding normal tissue. One of the physicians reviewed and analyzed all cases after a 2-week washout period.

The characteristic of suspicious colorectal lesions was diagnosed according to the location, shape, size, radioactivity distribution, and standardized uptake value (SUV) of the lesions. The semi-automatic quantitative measurements started with a manually placed elliptical working frame, which was drawn large enough to include the primary lesion, and manual adjustment was performed to exclude adjacent lymph nodes, metastatic lesions, and high physiologic uptake organs (**Figure 2**). The SUV_{max} and SUV_{peak} would be automatically calculated and generated after the placement of the working frame. Afterwards, a three-dimensional volume of interest (VOI) would be automatically outlined with chosen threshold within the working frame. According to previous studies, two common methods were selected to set the threshold. The first one was using the fixed threshold, also known as fixed absolute threshold; the thresholds of 2.5, 3.0, 4.0, and 5.0 were applied [18, 19]. The second approach was using the percent threshold, also known as fixed percentage threshold, setting the threshold between 30% and 60% with an increment of 10% of the SUV_{max} [20, 21]. With different thresholds, metabolic tumor volume (MTV), and SUV_{mean} could be identified inside the segmented VOI. Additionally, total lesion glycolysis (TLG) was calculated by MTV multiplying SUV_{mean} (TLG = MTV × SUV_{mean}), with representative images shown in **Figures 3**, **4**.

Immunohistochemical Evaluation

All patients underwent surgical resection within 3 months of PET/CT examination. The conventional HE and immunohistochemical staining of resected specimens were evaluated by a senior pathologist in a blind fashion. Specifically, the general pathological types, differentiation grade, TNM stages, and the expression of MMR proteins (MLH1, PMS2, MSH2, and MSH6) were assessed.

Proficient mismatch repair (pMMR) was identified when all of the four proteins were intact and expected to be microsatellite stable (MSS). On the contrary, those with the loss of one or more abovementioned MMR proteins were referred to as defective mismatch repair (dMMR) and characterized as MSI.

Statistical Analysis

The continuous variables were first checked for normality. The normally distributed data were expressed as the mean ± standard deviation (SD) and the difference was analyzed by Student's t test, while the data were expressed as medians and interquartile ranges and tested by Mann–Whitney U-test if not normally distributed. The categorical variables were shown as the number of cases and percentages, and compared by chi-squared test (or Fisher's exact test).

All quantitative PET/CT parameters were tested for inter-observer agreement and intra-observer agreement by interclass correlation coefficient (ICC) analysis, and ICC value greater than 0.90 was regarded as excellent agreement; between 0.75 and 0.90 as good agreement; between 0.5 and 0.75 as moderate agreement; and less than 0.50 as poor agreement. Receiver operating characteristic (ROC) analysis and the area under the ROC

FIGURE 2 | The workflow of ^{18}F-FDG PET/CT metabolic parameter measurements.
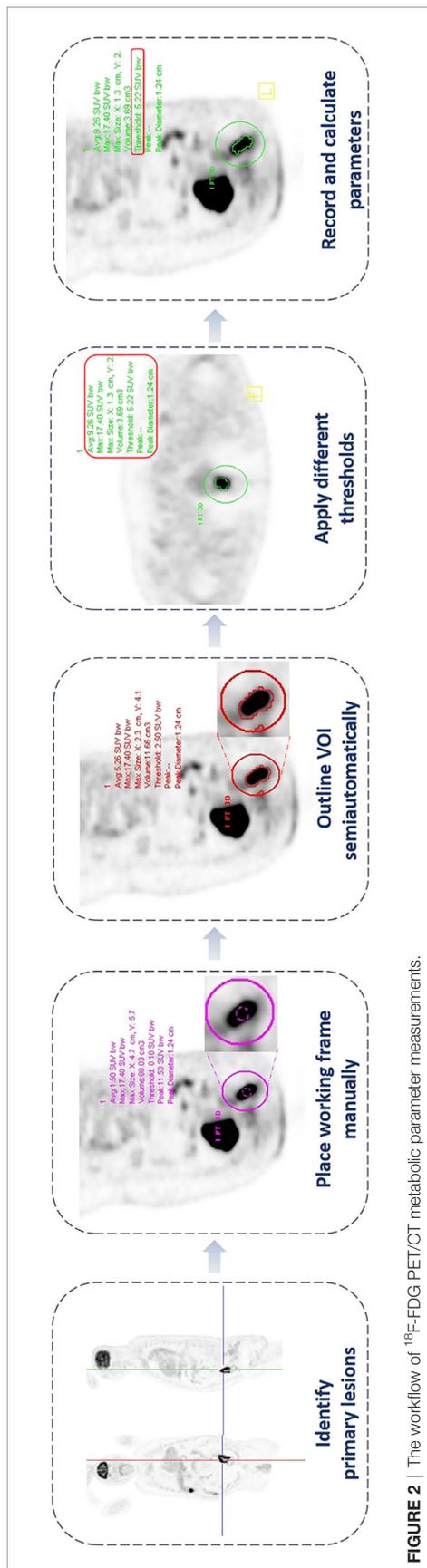
curve (AUC) were used to compare the predictive capabilities of quantitative PET/CT parameters between MSI and MSS group, and the sensitivity, specificity, optimal cutoff value, and 95% confidence interval (CI) were also calculated for each parameter. The comparison of different AUCs was conducted by the method described by DeLong et al. (22). Significant clinicopathological factors and the metabolic parameters with highest AUCs were entered into the multivariate logistic regression analysis.

All statistical analysis was performed by using SPSS software (version 22.0 IBM Corp, Armonk, NY) and MedCalc software (version 15.8). Two-sided p-values less than 0.05 were considered statistically significant.

RESULTS

Patient Characteristics
A total of 44 patients were finally enrolled in this study (24 males, 20 females, age range 28–90 years, median age 73 years), with 14 patients in the MSI group and 30 patients in the MSS group. In the current cohort, patients in the MSI group were older and their tumors appeared more often in the colon than the MSS group. There was no difference in TNM stage, pathological general types, differentiation grade, and tumor size between two groups. Detailed patient information and clinicopathological characteristics are listed in **Table 1**.

Inter-Observer and Intra-Observer Agreement of PET/CT Parameters
The excellent inter-observer and intra-observer agreement was found in SUV_{max} and SUV_{peak} with ICC values ranging from 0.999 to1.000. Other quantitative parameters also showed excellent inter-observer and intra-observer agreement with ICC values ranging from 0.958 to 0.999.

Difference of PET/CT Parameters in MSI and MSS Groups
The detailed SUV_{max}, SUV_{peak}, SUV_{mean}, MTV, and TLG in MSI and MSS groups are demonstrated in **Tables 2**, **3**. Specifically, MTVs were larger in CRC patients with MSI, with $MTV_{30\%}$, $MTV_{40\%}$, $MTV_{50\%}$, and $MTV_{60\%}$ showing significant difference (all p-values <0.05). Moreover, $TLG_{50\%}$ and $TLG_{60\%}$ were significantly larger in the MSI group than in the MSS group (all p-values <0.05). No significant difference was found in SUV_{max}, SUV_{peak}, and SUV_{mean} between two groups.

Predictive Performance of PET/CT and Clinical Parameters for MSI
For PET/CT parameters, $MTV_{50\%}$ demonstrated the highest predictive performance among the metabolic parameters, although not in a significant statistical way (all p-values >0.050), with an AUC of 0.805 (95% CI: 0.657–0.909), a sensitivity of 92.9% (95% CI: 0.661–0.998), and a specificity of 66.7% (95% CI: 0.472–0.827), respectively. The detailed predictive performance of PET/CT parameters and its ROC curves is illustrated in **Table 4** and **Figure 5**. For clinical parameters, the AUCs of age and tumor
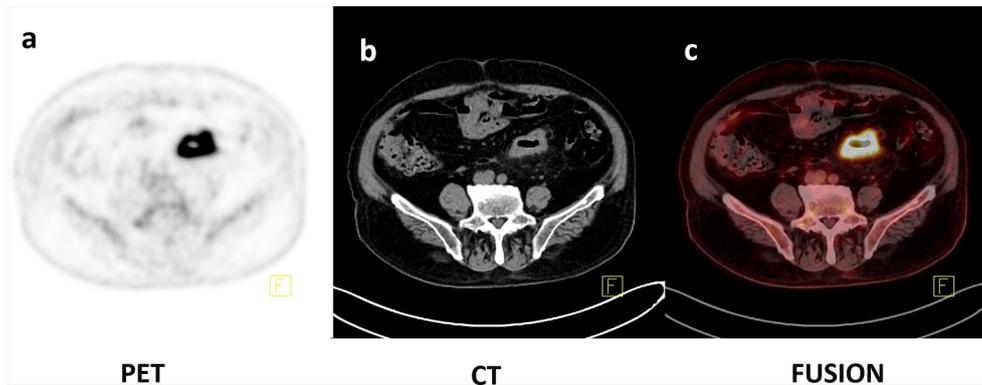
FIGURE 3 | Axial PET, CT, and fusion images of an 86-year-old female with histopathologically proven CRC with MSI **(A–C)**. ^{18}F-FDG PET/CT images showed that intense uptake in the sigmoid colon (SUV_{max} = 22.59, SUV_{peak} = 15.91, $SUV_{mean50\%}$ = 14.22, $MTV_{50\%}$ = 13.23 ml, $TLG_{50\%}$ = 188.13).
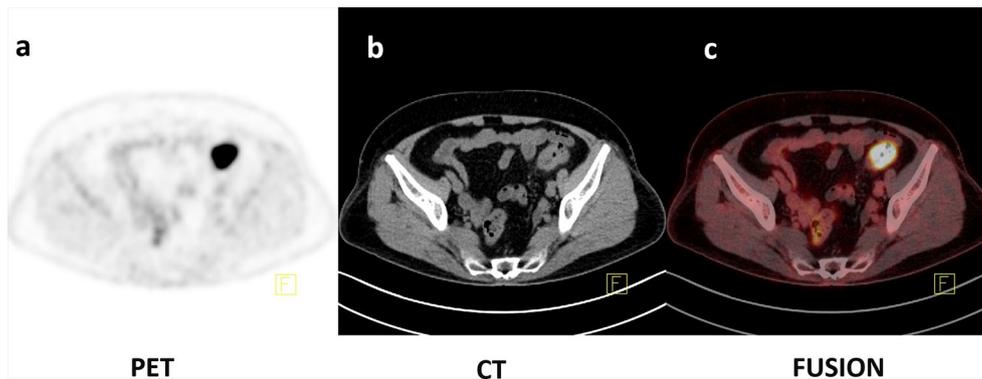
FIGURE 4 | Axial PET, CT, and fusion images of a 77-year-old female with histopathologically proven CRC with MSS **(A–C)**. ^{18}F-FDG PET/CT images showed that intense uptake in the sigmoid colon (SUV_{max} = 22.58, SUV_{peak} = 15.13, $SUV_{mean50\%}$ = 14.64, $MTV_{50\%}$ = 5.63 ml, $TLG_{50\%}$ = 82.4).

location were 0.843 (95% CI: 0.702–0.935) and 0.681 (95% CI: 0.523–0.813), respectively. No significant difference was found between AUCs of clinical and metabolic parameters (all $p >$ 0.050). In multivariate logistic regression, age, tumor location, and metabolic parameters were entered. To avoid multicollinearity, we only selected one significant metabolic parameter in each category for assessment, which were $MTV_{50\%}$ and $TLG_{60\%}$. The odds ratio and p-value of age, tumor location, $MTV_{50\%}$, and $TLG_{60\%}$ were 0.819 (p = 0.005), 20.460 (p = 0.059), 0.831 (p = 0.039), and 1.008 (p = 0.276), respectively, which suggested age and $MTV_{50\%}$ as the independent predictive indicators for MSI.

DISCUSSION

The current study revealed that age, tumor location, and certain metabolic parameters with specific thresholds had a significant difference between the MSI and MSS groups in patients with

CRC. MTV and TLG with higher percentage thresholds showed good predictive ability in identifying MSI, especially the $MTV_{50\%}$.

With the advancement of image analysis technology, MTV and TLG, which are volumetric indexes derived from ^{18}F-FDG PET, have been proposed for risk stratification of cancer patients (23). TLG is calculated by multiplying MTV by the SUV_{mean} of all voxels in the MTV, and represents both the degree of ^{18}F-FDG uptake and the size of the tumor. In other words, MTV is affected by tumor size and the distribution of the SUV, and TLG is affected by the whole metabolic and volumetric burden of the tumor (24–26). In fact, MTV and TLG were considered to be more reliable markers reflecting tumor burden and aggressiveness, as these indexes provide tumor burden information and additional information that takes into account intra-tumoral biologic variation. In the current study, we found that MTV and TLG were significantly different between MSI and MSS groups, which was in agreement with the previous findings (27). Jiang et al. (27) retrospectively analyzed the pretreatment parameters of PET and reported the highest diagnostic performance of $MTV_{3.0}$ and $TLG_{3.0}$ in predicting

TABLE 1 | Clinicopathological characteristics of included patients.

Characteristics	Overall (n = 44)	MSI (n = 14)	MSS (n = 30)	p-value
Sex				
Male	24	6	18	0.342
Female	20	8	12	
Age (years)[a]	71.1 ± 14.2	81.4 ± 8.5	66.3 ± 13.8	0.001
Tumor size (cm)[b]	5 (3.6, 6)	5.25 (4.63,7.25)	4.5 (3.15,5.5)	0.351
Tumor location				
Colon	30	13	17	0.019
Rectum	14	1	13	
Pathological general types				
Mass type	10	2	8	0.462
Ulcer type	34	12	22	
Differentiation grade				
Well or Moderate	29	7	22	0.177
Poor or	15	7	8	
Mucinous				
AJCC-TNM stage				
I–II	16	7	9	0.313
III–IV	28	7	21	
T stage				
T1–2	5	1	4	1.000
T3–4	38	12	26	
N stage				
Negative	20	9	11	0.112
Positive	24	5	19	
M stage				
Negative	29	11	18	0.314
Positive	15	3	12	

[a]*Data are presented in mean ± standard deviation (SD).*
[b]*data are presented in median (25th, 75th percentiles).*
MSI, microsatellite instability; MSS, microsatellite stability; AJCC, American Joint Committee on Cancer.

PD-L1 expression level in CRC. On the contrary, SUV_{max}, SUV_{peak}, and SUV_{mean} did not show a significant difference between MSI and MSS groups in the current study. SUV_{max} and SUV_{peak} only represent certain parts of the tumor and reflect the maximum extent of glucose metabolism within tumor cells (28), while SUV_{mean} was the average of tumor glucose uptake value. Therefore, SUV itself provides limited information on tumor lesion, and heterogeneity might not be accurately shown by the SUV values.

The present study found that patients' age and $MTV_{50\%}$ were significant predictive indicators of MSI, which was in agreement with a previous study (29) showing that CRC patients with MSI tended to be older. Similarly, Taieb et al. found that older age was associated with shorter survival after CRC recurrence (30). In addition, the predictive value of MTV with a higher percentage threshold tended to show better performance although not in a statistical way, which may due to the small sample size of the MSI group. Recent studies also confirmed that the different thresholds of MTV would affect the diagnostic performance. Bang's study (21) found that MTV calculated using various thresholds was significantly associated with the 3-year disease-free survival (DFS) rate of locally advanced rectal cancer, and MTV calculated using a higher threshold (40%–70% SUV_{max}) tended to be more strongly associated with 3-year DFS. In another study, various thresholds of metabolic parameters from FDG PET/CT were obtained and analyzed, and they found that $TLG_{40\%}$ can predict the treatment outcome of regorafenib in metastatic CRC (25). Moreover, we found that MTV with the percentage thresholds, rather than the fixed thresholds, showed better predictive performances of MSI

TABLE 2 | SUV measurements of CRC patients.

	SUV_{max}	SUV_{peak}	SUV_{mean} with fixed threshold method				SUV_{mean} with percent threshold method			
			2.5	3.0	4.0	5.0	30%	40%	50%	60%
MSI	19.34 ± 8.67	14.80 ± 6.01	6.94 ± 1.90	7.61 ± 2.12	8.61 ± 2.27	9.35 ± 2.38	9.83 ± 4.0	11.08 ± 4.35	12.34 ± 4.90	13.72 ± 5.61
MSS	21.43 ± 10.14	16.03 ± 8.35	6.97 ± 2.02	7.55 ± 2.15	8.62 ± 2.31	9.54 ± 2.45	10.77 ± 5.09	12.34 ± 5.84	13.94 ± 6.63	15.56 ± 7.46
p-value	0.509	0.821	0.965	0.929	0.986	0.806	0.549	0.476	0.427	0.417

MSI, microsatellite instability; MSS, microsatellite stability.

TABLE 3 | MTV and TLG measurements of CRC patients.

	MTV with fixed threshold method				MTV with percent threshold method			
	2.5	3.0	4.0	5.0	30%	40%	50%	60%
MSI	72.0 (41.93,80.8)	62.97 (33.29,70.65)	50.92 (24.13,57.83)	41.60 (18.52,49.96)	38.24 (23.27,48.34)	27.38 (14.65,33.86)	17.40 (10.19,24.12)	10.16 (6.46,16.78)
MSS	40.21 (23.14,78.87)	34.12 (19.54,70.73)	25.83 (14.73,59.71)	20.37 (11.64,43.42)	17.90 (12.0,36.89)	11.79 (8.59,22.87)	7.49 (4.94,13.51)	4.45 (2.76,7.93)
p-value	0.087	0.101	0.182	0.158	0.005	0.002	0.001	0.002

	TLG with fixed threshold method				TLG with percent threshold method			
	2.5	3.0	4.0	5.0	30%	40%	50%	60%
MSI	475.16 (209.33,632.36)	450.89 (209.33,632.36)	409.11 (178.06,582.65)	367.12 (156.62,546.46)	371.17 (185.63,474.80)	283.05 (137.02,413.55)	178.77 (106.44,335.98)	110.23 (69.57,228.48)
MSS	256.12 (136.95,600.94)	238.44 (129.04,578.47)	211.22 (114.0,528.22)	186.83 (100.83,476.36)	167.66 (105.18,167.66)	124.57 (86.95,316.87)	83.31 (68.57,223.38)	54.92 (43.47,105.0)
p-value	0.208	0.226	0.208	0.208	0.091	0.07	0.028	0.022

MSI, microsatellite instability; MSS, microsatellite stability; MTV, metabolic tumor volume; TLG, total lesion glycolysis.

TABLE 4 | Predictive performance of metabolic parameters.

Parameters	AUC (95% CI)	Optimal cutoff value	Sensitivity (95% CI)	Specificity (95% CI)
MTV $_{30\%}$	0.764 (0.612,0.879)	19.27	0.857 (57.2–98.2)	0.600 (40.6–77.3)
MTV $_{40\%}$	0.795 (0.647,0.902)	13.25	0.929 (66.1–99.8)	0.600 (40.6–77.3)
MTV $_{50\%}$	0.805 (0.657,0.909)	8.89	0.929 (66.1–99.8)	0.667 (47.2–82.7)
MTV $_{60\%}$	0.795 (0.647,0.902)	5.62	0.929 (66.1–99.8)	0.667 (47.2–82.7)
TLG $_{50\%}$	0.707 (0.549,0.865)	97.02	0.857 (57.2–98.2)	0.600 (40.6–77.3)
TLG $_{60\%}$	0.717 (0.561,0.842)	74.11	0.786 (49.2–95.3)	0.600 (40.6–77.3)

AUC, area under the ROC curve; CI, confidence interval; MTV, metabolic tumor volume; TLG, total lesion glycolysis.

FIGURE 5 | Receiver operating characteristic curves of MTV $_{30\%}$, MTV $_{40\%}$, MTV $_{50\%}$, and MTV $_{60\%}$ as well as TLG $_{50\%}$ and TLG $_{60\%}$ derived from PET/CT images for predicting MSI in CRC patients. The AUCs for predicting MSI from MSS were 0.764, 0.795, 0.805, and 0.795 for MTV $_{30\%}$, MTV $_{40\%}$, MTV $_{50\%}$, and MTV $_{60\%}$, respectively. In addition, the AUCs were 0.707 and 0.717 for TLG $_{50\%}$ and TLG $_{60\%}$.
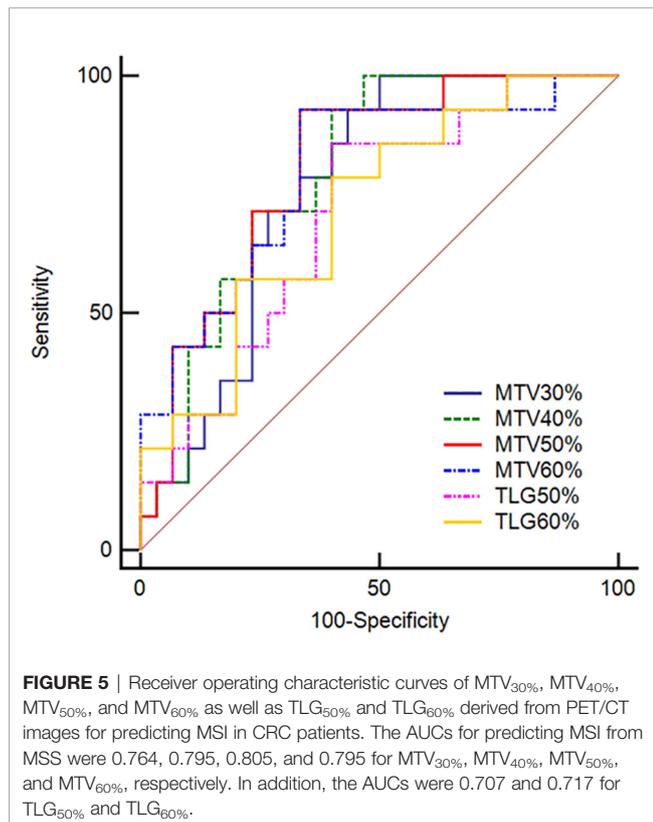
status in patients with CRC. Previous studies also demonstrated percentage thresholds method as a better way of measurements, as it was easily evaluated semiquantitative measurement of tumor textural heterogeneity and could minimize individual variations (19, 21). In addition, Henriksson et al. found the association between FDG uptake and the intra-tumoral heterogeneity in nude mice (31). On the other hand, Smedt et al. reported significant higher levels of cytotoxic T cells in the tumor and peritumoral region of MSI compared with MSS tumors (32). Therefore, MTV calculated using a higher threshold might be a representative

marker for tumor clinicopathological characteristics in patients with CRC.

We acknowledged several limitations in our study. First, there may be selection bias due to the retrospective nature of this study. Second, the sample size was limited in this study, and further validation is required by including a large cohort. Finally, our results were obtained from a single institution, and further multicenter investigations are needed to validate the utility of these metabolic parameters for predicting MSI in patients with CRC.

In conclusion, the metabolic parameters derived from ^{18}F-FDG PET/CT were able to preoperatively predict the MSI status in CRC, with MTV $_{50\%}$ demonstrating the highest predictive performance. Using these parameters, the noninvasive evaluation of MSI can be achieved, and thus better guiding immunotherapy in CRC patients.

DATA AVAILABILITY STATEMENT

The raw data supporting the conclusions of this article will be made available by the authors, without undue reservation.

ETHICS STATEMENT

The studies involving human participants were reviewed and approved by West China Hospital, Sichuan University. Written informed consent for participation was not required for this study in accordance with the national legislation, and the institutional requirements.

AUTHOR CONTRIBUTIONS

HL, TY, and BS contributed to conception and design of the study. HL and HX organized the image database and performed quantitative measurements. ZY, TD and ML performed the statistical analysis. HL and TY wrote the first draft of the manuscript. ZY, MW and BS revised the manuscript. All authors contributed to manuscript revision and read and approved the submitted version.

REFERENCES

1. Bray F, Ferlay J, Soerjomataram I, Siegel RL, Torre LA, Jemal A. Global Cancer Statistics 2018: GLOBOCAN Estims of Incidence and Mortality

Worldwide for 36 Cancers in 185 Countries. *CA: Cancer J Clin* (2018) 68 (6):394–424. doi: 10.3322/caac.21492

2. Kuipers EJ, Grady WM, Lieberman D, Seufferlein T, Sung JJ, Boelens PG, et al. Colorectal Cancer. *Nat Rev Dis Primers* (2015) 1:15065. doi: 10.1038/nrdp.2015.65

3. Lichtenstern CR, Ngu RK, Shalapour S, Karin M. Immunotherapy, Inflammationand Colorectal Cancer. *Cells* (2020) 9(3):618. doi: 10.3390/cells9030618

4. Pardoll DM. The Blockade of Immune Checkpoints in Cancer Immunotherapy. *Nat Rev Cancer* (2012) 12(4):252–64. doi: 10.1038/nrc3239

5. Brudvik KW, Røsok B, Naresh U, Yaqub S, Fretland ÅA, Labori KJ, et al. Survival After Resection of Colorectal Liver Metastases in Octogenarians and Sexagenarians Compared to Their Respective Age-Matched National Population. *Hepatobiliary Surg Nutr* (2018) 7(4):234–41. doi: 10.21037/hbsn.2017.09.03

6. Grady WM, Carethers JM. Genomic and Epigenetic Instability in Colorectal Cancer Pathogenesis. *Gastroenterology* (2008) 135(4):1079–99. doi: 10.1053/j.gastro.2008.07.076

7. Passardi A, Canale M, Valgiusti M, Ulivi P. Immune Checkpoints as a Target for Colorectal Cancer Treatment. *Int J Mol Sci* (2017) 18(6):1324. doi: 10.3390/ijms18061324

8. Sargent DJ, Marsoni S, Monges G, Thibodeau SN, Labianca R, Hamilton SR, et al. Defective Mismatch Repair as a Predictivemarker for Lack of Efficacy of Fluorouracil-Based Adjuvant Therapy in Coloncancer. *J Clin Oncol* (2010) 28 (20):3219–26. doi: 10.1200/JCO.2009.27.1825

9. Romiti A, Rulli E, Pilozzi E, Gerardi C, Roberto M, Legramandi L, et al. Exploring the Prognostic Role Ofmicrosatellite Instability in Patients With Stage II Colorectal Cancer: ASystematic Review and Meta-Analysis. *Clin Colorectal Cancer* (2017) 16(2):e55–9. doi: 10.1016/j.clcc.2016.08.007

10. Shia J. Immunohistochemistry Versus Microsatellite Instability Testing Forscreening Colorectal Cancer Patients at Risk for Hereditary Nonpolyposiscolorectal Cancer Syndrome. Part I. The Utility of Immunohistochemistry. *J Mol Diagn* (2008) 10 (4):293–300. doi: 10.2353/jmoldx.2008.080031

11. Sun R, Limkin EJ, Vakalopoulou M, Dercle L, Champiat S, Han SR, et al. A Radiomics Approach Toassess Tumour-Infiltrating CD8 Cells and Response to Anti-PD-1 or Anti-PD-L1immunotherapy: An Imaging Biomarker, Retrospective Multicohort Study. *Lancet Oncol* (2018) 19(9):1180–91. doi: 10.1016/S1470-2045(18)30413-3

12. Punt CJ, Koopman M, Vermeulen L. From Tumour Heterogeneity to Advances in Precision Treatment of Colorectal Cancer. *Nat Rev Clin Oncol* (2017) 14(4):235–46. doi: 10.1038/nrclinonc.2016.171

13. Wu J, Lv Y, Wang N, Zhao Y, Zhang P, Liu Y, et al. The Value of Single-Source Dual-Energy CT Imaging for Discriminating Microsatellite Instability From Microsatellite Stability Human Colorectal Cancer. *Eur Radiol* (2019) 29 (7):3782–90. doi: 10.1007/s00330-019-06144-5

14. Zhang W, Yin H, Huang Z, Zhao J, Zheng H, He D, et al. Development and Validation of MRI-Based Deep Learning Models for Prediction of Microsatellite Instability in Rectal Cancer. *Cancer Med* (2021) 10:4164–73. doi: 10.1002/cam4.3957

15. Meacham CE, Morrison SJ. Tumour Heterogeneity and Cancer Cell Plasticity. *Nature* (2013) 501(7467):328–37. doi: 10.1038/nature12624

16. Wu M, Zhang Y, Zhang Y, Liu Y, Wu M, Ye Z. Imaging-Based Biomarkers for Predicting and Evaluating Cancer Immunotherapy Response. *Radiol Imaging Cancer* (2019) 1(2):e190031. doi: 10.1148/rycan.2019190031

17. Kaira K, Higuchi T, Naruse I, Arisaka Y, Tokue A, Altan B, et al. Metabolic Activity by 18F-FDG-PET/CT Is Predictive of Early Response After Nivolumab in Previously Treated NSCLC. *Eur J Nucl Med Mol Imaging* (2018) 45(1):56–66. doi: 10.1007/s00259-017-3806-1

18. Im HJ, Bradshaw T, Solaiyappan M, Cho SY. Current Methods to Define MetabolicTumor Volume in Positron Emission Tomography: Which One Is Better? *Nucl Med Mol Imaging* (2018) 52(1):5–15. doi: 10.1007/s13139-017-0493-6

19. Suzuki Y, Okabayashi K, Hasegawa H, Tsuruta M, Shigeta K, Murakami K, et al. Metabolic Tumor Volume and Total Lesion Glycolysis in PET/CT Correlate With the Pathological Findings of Colorectal Cancer and Allow Its Accurate Staging. *Clin Nucl Med* (2016) 41(10):761–5. doi: 10.1097/RLU.0000000000001332

20. Mapelli P, Bergamini A, Fallanca F, Rancoita PMV, Cioffi R, Incerti E, et al. Prognosticrole of FDG PET-Derived Parameters in Preoperative Staging of Endometrialcancer. *Rev Esp Med Nucl Imagen Mol (Engl Ed)* (2019) 38(1):3–9. doi: 10.1016/j.remn.2018.06.007. English,Spanish.

21. Bang JI, Ha S, Kang SB, Lee KW, Lee HS, Kim JS, et al. Prediction of Neoadjuvant Radiation Chemotherapy Response and Survival Using Pretreatment [(18)F]FDG PET/CT Scans in Locally Advanced Rectal Cancer. *Eur J Nucl Med Mol Imaging* (2016) 43(3):422–31. doi: 10.1007/s00259-015-3180-9

22. DeLong ER, DeLong DM, Clarke-Pearson DL. Comparing the Areas Under Two Ormore Correlated Receiver Operating Characteristic Curves: A Nonparametricapproach. *Biometrics* (1988) 44(3):837–45. doi: 10.2307/2531595

23. Romesser PB, Qureshi MM, Shah BA, Chatburn LT, Jalisi S, Devaiah AK. Superior Prognostic Utility of Gross and Metabolic Tumor Volume Compared to Standardized Uptake Value Using PET/CT in Head and Neck Squamous Cell Carcinoma Patients Treated With Intensity-Modulated Radiotherapy. *Ann Nucl Med* (2012) 26(7):527–34. doi: 10.1007/s12149-012-0604-5

24. Moon SH, Hyun SH, Choi JY. Prognostic Significance of Volume-Based PET Parameters in Cancer Patients. *Korean J Radiol* (2013) 14(1):1–12. doi: 10.3348/kjr.2013.14.1.1

25. Lim Y, Bang JI, Han SW, Paeng JC, Lee KH, Kim JH, et al. Total Lesion Glycolysis (TLG) as an Imaging Biomarker in Metastatic Colorectal Cancer Patients Treated With Regorafenib. *Eur J Nucl Med Mol Imaging* (2017) 44 (5):757–64. doi: 10.1007/s00259-016-3577-0

26. Rahim MK, Kim SE, So H, Kim HJ, Cheon GJ, Lee ES, et al. Recent Trends in PET Image Interpretations Using Volumetric and Texture-Based Quantification Methods in Nuclear Oncology. *Nucl Med Mol Imaging* (2014) 48(1):1–15. doi: 10.1007/s13139-013-0260-2

27. Jiang H, Zhang R, Jiang H, Zhang M, Guo W, Zhang J, et al. Retrospective Analysis of the Prognostic Value of PD-L1 Expression and 18F-FDG PET/CT Metabolic Parameters in Colorectal Cancer. *J Cancer* (2020) 11(10):2864–73. doi: 10.7150/jca.38689

28. Im HJ, Pak K, Cheon GJ, Kang KW, Kim SJ, Kim IJ, et al. Prognostic Value of Volumetric Parameters of (18)F-FDG PET in Non-Small-Cell Lung Cancer: A Meta-Analysis. *Eur J Nucl Med Mol Imaging* (2015) 42(2):241–51. doi: 10.1007/s00259-014-2903-7

29. Fujiyoshi K, Yamaguchi T, Kakuta M, Takahashi A, Arai Y, Yamada M, et al. Predictive Model for High-Frequency Microsatelliteinstability in Colorectal Cancer Patients Over 50 Years of Age. *Cancer Med* (2017) 6(6):1255–63. doi: 10.1002/cam4.1088

30. Taieb J, Shi Q, Pederson L, Alberts S, Wolmark N, Van Cutsem E, et al. Prognosis of Microsatellite Instability and/or Mismatch Repairdeficiency Stage III Colon Cancer Patients After Disease Recurrence Following adjuvant Treatment: Results of an ACCENT Pooled Analysis of Seven Studies. *Ann Oncol* (2019) 30(9):1466–71. doi: 10.1093/annonc/mdz208

31. Henriksson E, Kjellen E, Wahlberg P, Ohlsson T, Wennerberg J, Brun E. 2-Deoxy-2-[18F] Fluoro-D-Glucose Uptake and Correlation to Intratumoral Heterogeneity. *Anticancer Res* (2007) 27(4B):2155–9.

32. De Smedt L, Lemahieu J, Palmans S, Govaere O, Tousseyn T, Van Cutsem E, et al. Microsatellite Instable vs Stable Colon Carcinomas: Analysis of Tumour Heterogeneity, Inflammation and Angiogenesis. *Br J Cancer* (2015) 113 (3):500–9. doi: 10.1038/bjc.2015.213